Adaptronic Vibration Absorber for a Wide Field of Applications

Authors: ***Pietro Pagliarulo, Klaus Kuhnen and Hartmut Janocha***
Laboratory of Process Automation (LPA), Saarland University, Saarbruecken, Germany. E-Mail: p.pagliarulo@lpa.uni-saarland.de

Unwanted externally excited or self-induced vibrations occurring in many mechanical structures of our engineered environment need to be reduced in the interest of lower environmental impact and increased structural durability. Reducing vibrations can be achieved with the help of passive vibration absorbers, which extract kinetic energy from the vibrating host system, or active ones, which introduce opposing forces into the structure to affect compensation. Focusing on an auxiliary mass damper, this paper shows how both classes of absorber can be unified in a single, compact unit through the use of active materials and an adaptronic system approach. Simulation and experimental results corresponding to a particular technical application illustrate broadband damping of time varying frequency components in the spectrum of structural vibrations.

1 Introduction

Unwanted vibrations often occur in airplanes, trains, machine tools and other mechanical structures. One tries to avoid or at least reduce these structural vibrations with the objective of eliminating danger to humans and machines, lowering environmental impact (noise) and increasing structural durability of systems as well as enhancing the quality of technical products and processes.

Vibration reduction is achieved, for example, by applying vibration absorbers with auxiliary masses which, as is generally known, can be divided into passive and active systems. Passive systems transform the disturbing vibrational energy of the main structure into another form of energy (e.g. heat). They are of simple construction but only effective over a small frequency range [1,2]. Active systems, however, transmit a compensating "counter force" into the vibrating structure; they have a broadband effect, but are much more complex [3].

This paper describes an auxiliary mass damper that has been developed within the European project MESA [9] and optimized within the European project MESEMA [12] and that can work either passively or actively (patent DE 103 21 436). The natural frequency and damping properties in the former case can be tuned electrically: semi-active damper [5]. A particular property of the described damper version is the high function density typical of adaptronic devices [3]. Furthermore, the sensory and actuator properties of so-called active materials, being also part of the auxiliary mass, are exploited. The following sections 2 to 5 focus on the basic theory of such an auxiliary mass damper where highly magnetostrictive and piezoelectric materials are applied as active materials. Section 6 describes the reduction of structural vibrations comparing the measured operating behaviour of a real damper with the theoretical predictions (simulations) within the context of application in turbo-prop airplanes [14].

2 Passive Auxiliary Mass Damper

Consider an effective mass m_1 that is acted upon by an equivalent excitation force $F_1(t) = m_1 a_1(t)$ leading to a local acceleration amplitude $a_1(t) = \mathrm{d}^2 s_1(t)/\mathrm{d}t^2$. The purpose of an auxiliary mass damper, as apparent in Figure 1, is to generate a secondary force $F_2 = F_c + F_d$ that compensates the primary force F_1 thereby counteracting the excitation of mass m_1.

In the Laplace domain (where $p = \sigma + \mathrm{j}\omega$) the following constant disturbance transfer function for the motion of the effective mass m_1 can be derived from Figure 1.

$$G_D(p) = \frac{a_1(p)}{F_1(p)} = \frac{1}{m_1} \qquad (1)$$

In the case of a narrowband primary force the vibrations can be dampened by the passive auxiliary mass damper described in Figure 1.

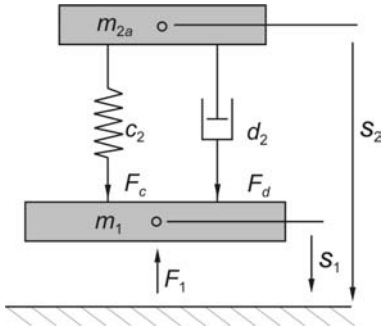

Figure 1: *Effective mass m_1 with primary force excitation F_1 and passive auxiliary mass damper m_{2a}, c_2, d_2*

In its most simple form, an auxiliary mass damper consists of an auxiliary mass m_{2a} which is coupled to the primary system via a spring element with the stiffness c_2 and a damping element with the damping factor d_2. Beginning with the equations of motion for the two masses m_1 and m_{2a} the equation for the disturbance transfer function of the effective mass m_1 becomes

$$G_D(p) = \frac{a_1(p)}{F_1(p)} = +K_D \frac{\frac{1}{\omega_a^2}p^2 + \frac{2D_a}{\omega_a}p + 1}{\frac{1}{\omega_r^2}p^2 + \frac{2D_r}{\omega_r}p + 1} \qquad (2)$$

with

$$\omega_r = \sqrt{c_2 \frac{m_1 + m_{2a}}{m_1 m_{2a}}}\,,\quad D_r = \frac{1}{2} d_2 \sqrt{\frac{m_1 + m_{2a}}{c_2 m_1 m_{2a}}}\,,$$

$$\omega_a = \sqrt{\frac{c_2}{m_{2a}}}\,,\quad D_a = \frac{1}{2} d_2 \sqrt{\frac{1}{c_2 m_{2a}}}\,,\quad K_D = \frac{1}{m_1 + m_{2a}}\,.$$

In the undamped case ($d_2 = 0$) the denominator of transfer function (2) has a zero at $p = \mathrm{j}\omega_r$ for the frequency ω_r. In the field of structural dynamics this special frequency is defined as the resonant frequency. The numerator of transfer function (2) on the contrary exhibits a zero at $p = \mathrm{j}\omega_a$ for the resonant frequency ω_a of the passive auxiliary mass damper. At this particular frequency, the so-called anti-resonant frequency of the overall system (effective mass with damper), the effective mass m_1 cannot experience any motion, independent of the amplitude of the excitation force F_1. For this reason, the parameters auxiliary mass m_{2a} and spring stiffness c_2 are typically selected such that the anti-resonant frequency ω_a of the passive auxiliary mass damper corresponds with the dominating frequency component of the primary force F_1.

3 Semi-Active Auxiliary Mass Damper

In many applications with narrowband excitation of the effective mass the dominating primary force component is subject to operational-dependent frequency variations. A statically tuned auxiliary mass damper therefore cannot be optimally adapted to all possible operating conditions. In such cases the use of electrically controllable passive auxiliary mass dampers, which are often defined as semi-active auxiliary mass dampers in the literature, can be very advantageous [4]. Here, the auxiliary mass is coupled to the vibrating main system by electrically controllable materials such as piezoelectric or magnetostrictive materials. The mechanical parameters stiffness and damping of the passive auxiliary mass damper can then be influenced with help of actuator and sensory properties of the active materials and feedback of the actuator force. The basic approach to control the passive mechanical properties of active materials is described in Figure 2 considering as example an actuator-sensor combination consisting of two magnetostrictive rods and two piezoelectric plates [5]. The piezoelectric plates are placed between the two magnetostrictive rods. They assume a sensor function and produce a polarization charge q_s that, depending on the rod load F, can be identified with knowledge of the effective piezoelectric constant d_P for adequately small loads via the linear relationship

$$q_S(t) = d_P F(t)\,. \qquad (3)$$

The electromechanical model according to Figure 2b describes the sensor effect as a controlled current source with the source current $\mathrm{d}q_S/\mathrm{d}t$. The magnetostrictive rods perform a pure actuator function delivering a displacement depending on the driving current I, which for sufficiently small currents can be described by the linear relationship

$$s_A(t) = d_M I(t) \qquad (4)$$

where d_M is the effective magnetostrictive constant.

The electromechanical model according to Figure 2b describes the actuator effect as a controlled displacement source with the source active displacement s_A. The total displacement s of the actuator-sensor combination thus consists additively of a passive load-dependent part s_P and an active current-dependent part s_A. The relationship between the passive part s_P and the rod load F is given in a first approximation by

$$F(t) = c_P s_P(t) \qquad (5)$$

and is characterized by the passive stiffness c_P of the actuator-sensor combination in the model of Figure 2b.

3.1 Charge Amplifier

The charge of the piezoelectric plates is conditioned electrically by a charge amplifier that essentially consists of an integrated operational amplifier with high-impedance input and a capacitive feedback [6] and thus produces at the input a virtual short-circuit to ground. The relationship between charge q_S and output voltage U_{S1} is defined by the transfer function $U_{S1}(p) = G_{S1}(p)q_S(p)$ where

$$G_{S1}(p) = -K_{S1}\frac{p}{\tau_{S1}p + 1}\,. \qquad (6)$$

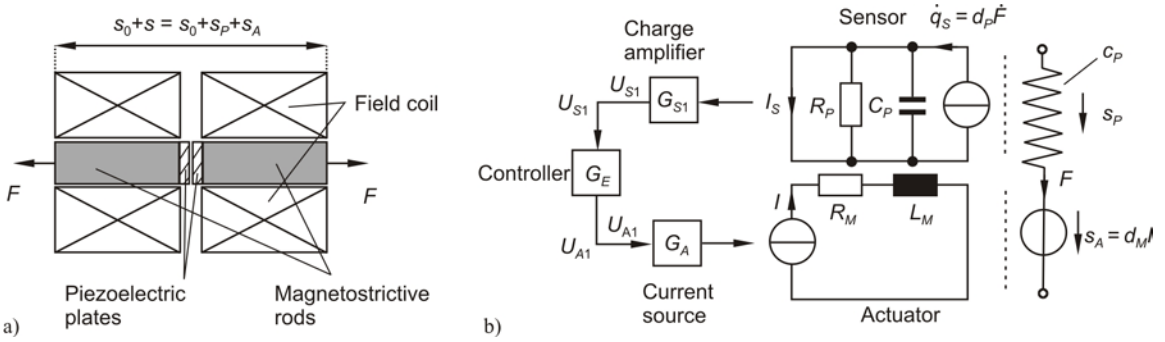

Figure 2: *Actuator-sensor combination: a) arrangement of magnetostrictive actuator rods and piezoelectric sensor plates, b) electromechanical model with control loop for regulating the mechanical behaviour*

The charge amplifier shows high-pass behaviour with the gain K_{S1}, the time constant τ_{S1} and the cut-off frequency $f_{S1} = 1/(2\pi\tau_{S1})$.

3.2 Power Current Source

The coil current for driving the two magnetostrictive actuator rods is generated by a voltage-controlled power current source. The transfer function $G_A(p) = I(p)/U_{A1}(p)$ of the current source is given in a first approximation by

$$G_A(p) = K_A \frac{1}{\tau_A p + 1}. \tag{7}$$

Thus, the power current source exhibits low-pass behaviour with the gain K_A, the time constant τ_A and the cut-off frequency $f_A = 1/(2\pi\tau_A)$.

3.3 Active Spring and Active Damper

If a transfer function $G_E(p) = U_{A1}(p)/U_{S1}(p)$ is implemented between the sensor output voltage U_{S1} and the input voltage of the current source, e.g. by means of an electronic circuit, the resulting overall mechanical behaviour of the actuator-sensor combination can be described by

$$s(p) = \left(\frac{1}{c_P} + d_M G_A(p) G_E(p) G_{S1}(p) d_P \right) F(p) \tag{8}$$

and thus influenced systematically by the transfer function $G_E(p)$ of the electronic circuit (controller). The following relationship between the displacement $s(p)$ and the force $F(p)$ can be obtained from the mechanical system model in Figure 3.

$$s(p) = \left(\frac{1}{c_P} + \frac{1}{c_A + d_A p} \right) F(p). \tag{9}$$

For frequencies $f_{S1} << f << f_A$ equation (8) can be simplified to

$$s(p) = \left(\frac{1}{c_P} - d_M K_A \frac{K_{S1}}{\tau_{S1}} d_P G_E(p) \right) F(p). \tag{10}$$

Comparing equations (9) and (10) leads to the transfer function for the electronic circuit

$$G_E(p) = -K_E \frac{1}{\tau_E p + 1} \tag{11}$$

where the gain and the time constant are

$$K_E = \frac{\tau_{S1}}{c_A d_M K_A K_{S1} d_P} \quad \text{and} \quad \tau_E = \frac{d_A}{c_A}.$$

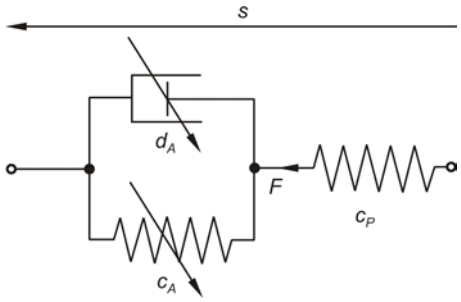

Figure 3*: Variable spring and damper [7]*

3.4 Displacement Amplification

The vibration attenuating effect of an auxiliary mass damper is stronger the greater its mass. However, too much additional mass alters the basic vibrating – and possibly even the functional – behaviour of the structure, which is undesired. As is evident in the relationship $F_2(t) = m_{2a}a_2(t)$, a lower added mass m_{2a} can achieve the necessary force F_2 for the desired vibration attenuation if the acceleration a_2 of the auxiliary mass is increased.

Considering harmonic operation of the system the relationship $|a_{20}| = \omega^2 s_{20}$ can be applied. Consequently, the auxiliary mass needed to generate a certain force amplitude at a certain frequency of the damper can only be minimized by increasing the displacement amplitude. Since the maximum strain of the magnetostrictive rods amounts to 0.1...0.2%, the achievable displacement of an auxiliary mass directly coupled to the active material with a given dimension of the actuator-

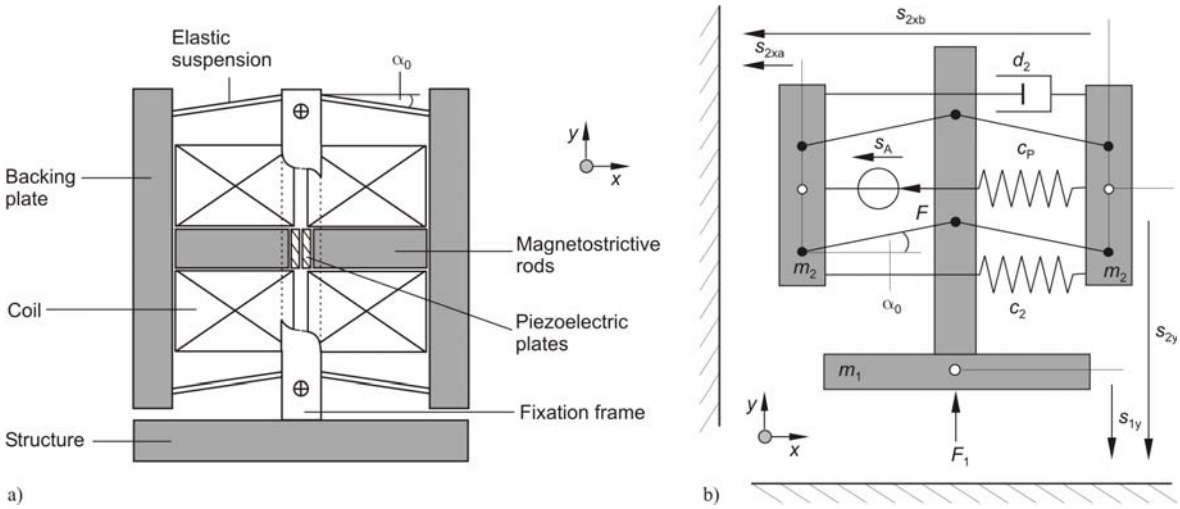

***Figure 4**: Magnetostrictive auxiliary mass damper with displacement amplifier: a) construction, b) mechanical model*

sensor combination is typically quite low. This contradiction can be resolved using displacement amplification systems based on rigid arms [8]. Since the auxiliary mass contributes directly to the total mass of the damper, the total mass can be reduced if the auxiliary mass is a preferably big part of the total mass.

Figure 4 illustrates a displacement amplification concept in which the displaced mass amounts to 90% of the total mass [9,5,10]. In this construction the primary extension of the actuator-sensor combination occurs in the longitudinal direction (*x*-axis). This displacement is transformed by the elastic suspension to a significantly larger motion of the auxiliary mass consisting of the magnetostrictive rods, the piezoelectric plates, the coils and the backing plates in the perpendicular direction (*y*-axis). The displacement amplification decisively depends on the angle α_0 of the elastic suspension and is greater the smaller this angle α_0 is chosen. All parts of the auxiliary mass damper except the fixation frame undergo motion in the desired effective direction. From this concept emerges therefore a very compact design that allows a very effective use of the installation space to produce the inertial force F_2.

Using the auxiliary mass damper shown in the mechanical model of Figure 4b a simplified model for simulations or for the control synthesis can be derived. In this mechanical model the displacement amplification is represented in a first approximation by two parallel rigid arms suspended at play-free and frictionless joints. The elasticity of the suspension that simultaneously provides the mechanical preload for the actuator-sensor combination is considered by the linear elastic spring with the stiffness c_2. The structural damping in this construction is represented by the linear viscous damper with the damping factor d_r. The mass of the backing plates, of the coils as well as of the effective parts of the suspension and of the actuator-sensor combination are concentrated in the two identical masses m_2, so that the moved auxiliary mass consists of the sum of both masses (here $m_{2a} = 2m_2$).

Linearization about the initial angle α_0 of the state equations describing the mechanical system and subsequent transformation into the Laplace domain leads after longer calculation to the relationships

$$F(p) = G_{FF}(p)s_A(p) + G_{SF}(p)F_1(p) \tag{12}$$

$$a_1(p) = G_{Fa}(p)s_A(p) + G_{Sa}(p)F_1(p) \tag{13}$$

between the base acceleration a_1 as well as the rod load F as output quantities and the primary force F_1 and the active displacement s_A as input quantities. The transfer functions are

$$G_{FF}(p) = \frac{F(p)}{s_A(p)} = -K_{FF}\frac{\frac{1}{\omega_{FF}^2}p^2 + \frac{2D_{FF}}{\omega_{FF}}p + 1}{\frac{1}{\omega_r^2}p^2 + \frac{2D_r}{\omega_r}p + 1}, \tag{14}$$

$$G_{Fa}(p) = \frac{a_1(p)}{s_A(p)} = -K_{Fa}\frac{p^2}{\frac{1}{\omega_r^2}p^2 + \frac{2D_r}{\omega_r}p + 1}, \tag{15}$$

$$G_{SF}(p) = \frac{F(p)}{F_1(p)} = -K_{SF}\frac{1}{\frac{1}{\omega_r^2}p^2 + \frac{2D_r}{\omega_r}p + 1}, \tag{16}$$

$$G_{Sa}(p) = \frac{a_1(p)}{F_1(p)} = +K_{Sa}\frac{\frac{1}{\omega_{Sa}^2}p^2 + \frac{2D_{Sa}}{\omega_{Sa}}p + 1}{\frac{1}{\omega_r^2}p^2 + \frac{2D_r}{\omega_r}p + 1} \tag{17}$$

with the parameters

$$\omega_r = \sqrt{2(c_2 + c_P)\frac{m_1 + 2m_2}{(1+\eta^2)m_1m_2 + 2m_2^2}},$$

$$D_r = \frac{1}{2} d_2 \sqrt{\frac{2}{c_2 + c_P} \frac{m_1 + 2m_2}{(1+\eta^2) m_1 m_2 + 2m_2^2}},$$

$$\omega_{FF} = \sqrt{2c_2 \frac{m_1 + 2m_2}{(1+\eta^2) m_1 m_2 + 2m_2^2}},$$

$$D_{FF} = \frac{1}{2} d_2 \sqrt{\frac{2}{c_2} \frac{m_1 + 2m_2}{(1+\eta^2) m_1 m_2 + 2m_2^2}},$$

$$\omega_{Sa} = \sqrt{2 \frac{c_2 + c_P}{(1+\eta^2) m_2}},$$

$$D_{Sa} = \frac{1}{2} d_2 \sqrt{\frac{2}{c_P + c_2} \frac{1}{(1+\eta^2) m_2}},$$

$$K_{FF} = \frac{c_2}{c_P + c_2} c_P,$$

$$K_{Sa} = \frac{1}{m_1 + 2m_2},$$

$$K_{SF} = \frac{c_P}{c_P + c_2} \frac{m_2}{m_1 + 2m_2} \eta,$$

$$K_{Fa} = \frac{c_P}{c_P + c_2} \frac{m_2}{m_1 + 2m_2} \eta$$

and the displacement amplification ratio at the operating point

$$\eta = \cot(\alpha_0).$$

3.5 Semi-Active Mode

The part of the model and the signal flow diagram of Figure 5 marked in light grey shows the configuration for the semi-active operating mode of the auxiliary mass damper.

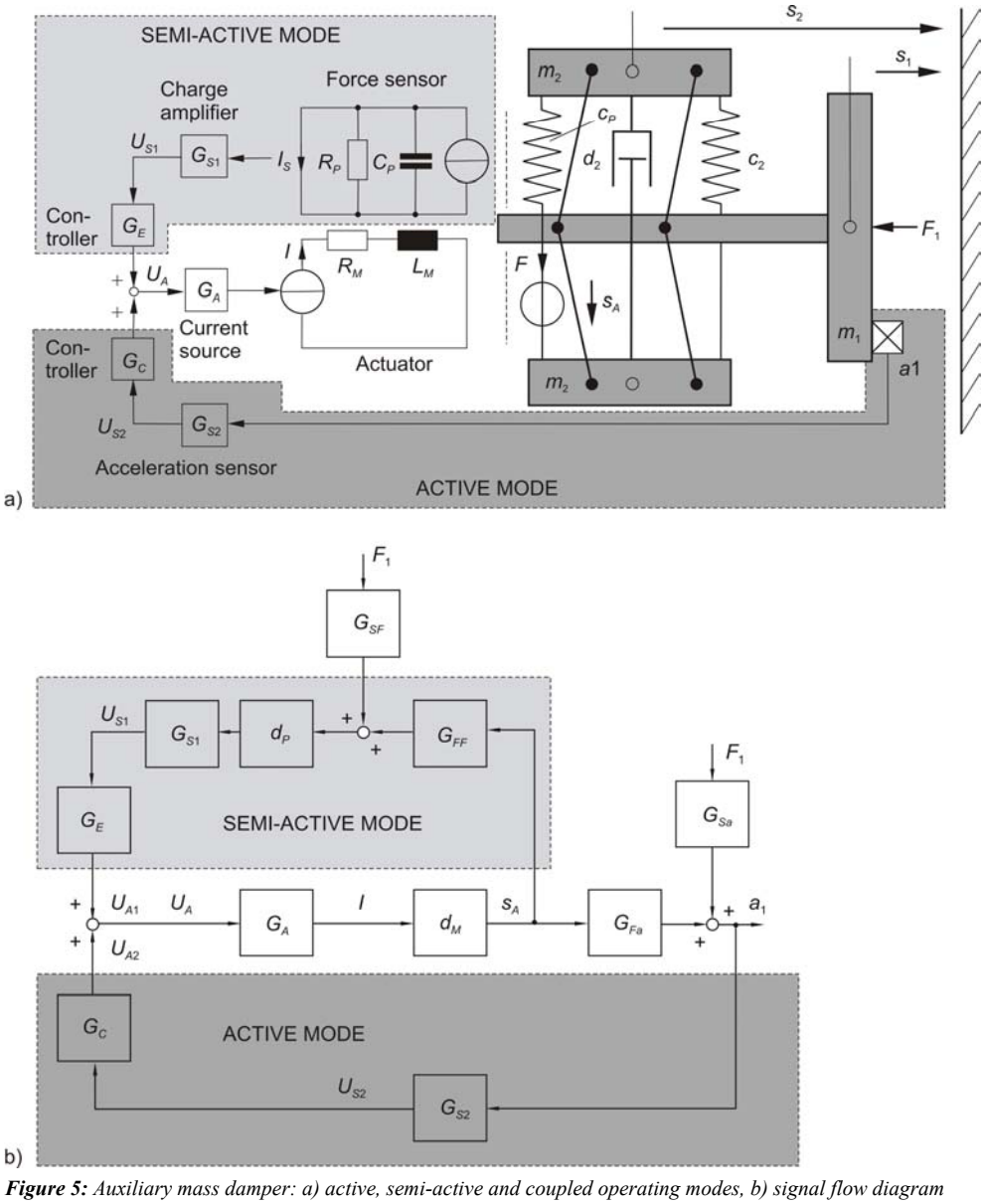

Figure 5: *Auxiliary mass damper: a) active, semi-active and coupled operating modes, b) signal flow diagram*

For this par the disturbance transfer function $G_D(p) = a_1(p)/F_1(p)$ in the semi-active mode is

$$G_D(p) = G_{Sa}(p) + G_{Fa}(p)G_{CL}(p)G_{SF}(p) \qquad (18)$$

with

$$G_{CL}(p) = \frac{d_P G_{S1}(p) G_E(p) G_A(p) d_M}{1 - d_P G_{S1}(p) G_E(p) G_A(p) d_M G_{FF}(p)} . \qquad (19)$$

The following simulations are based on a semi-active auxiliary mass damper characterised by the parameter values in Table 1. Figure 6a shows the dependence of the amplitude response of the disturbance transfer function on the variable c_A for $d_A = 0$. For $c_A >> c_P$, only the passive stiffness c_P together with c_2 is effective in the mechanical system and defines together with the masses m_1 and m_2 the location of the resonant and anti-resonant frequencies of the overall system. The greatest dependence of the locations of the resonant and anti-resonant frequencies on the active stiffness exists in the range $c_2 \geq c_A \geq c_P$. For $c_P >> c_A$ the active stiffness determines the mechanical behaviour of the actuator-sensor combination, and thus in the mechanical system only the stiffness c_2 of the preloading mechanism is effective. Another shift of the resonant and anti-resonant frequencies of the overall system is therefore impossible under this condition. Consequently the range of variability of the location of the resonant and anti-resonant frequencies of the overall system becomes wider the greater the passive stiffness of the actuator-sensor combination is in relation to the stiffness of the mechanical preload spring.

Parameter	Value	Unit
c_P	$1.5 \cdot 10^{+6}$	N/m
d_M	$40 \cdot 10^{-6}$	m/A
d_P	$680 \cdot 10^{-12}$	C/N
m_1	7	kg
m_2	0.15	kg
c_2	$4.5 \cdot 10^{+6}$	N/m
d_2	450	Ns/m
η	12	-
K_A	10	1/Ω
f_A	1	kHz
K_{S1}	2.34	MΩ
f_{S1}	1	Hz

***Table 1**: Parameter values of a semi-active auxiliary mass damper*

Figure 6b shows the dependence of the amplitude response of the disturbance transfer function on the variable d_A with $c_A = 0.015$ MN/m. As expected, for an increasing active damping factor one can observe a slight increase in the amplitude response within the region of the anti-resonant frequency and a slight decrease in the amplitude response within the region of the resonant frequency of the overall system. According to the explanations in section 3.3 a variation of c_A within the defined interval [0.15 MN/m ∞[corresponds to a variation of K_E in the range [1.67 0]; with $c_A = 0.015$ MN/m a variation of d_A within the defined range [10 Ns/m 1000 Ns/m] corresponds to a variation of τ_E in the range [0.00067 s 0.067 s].

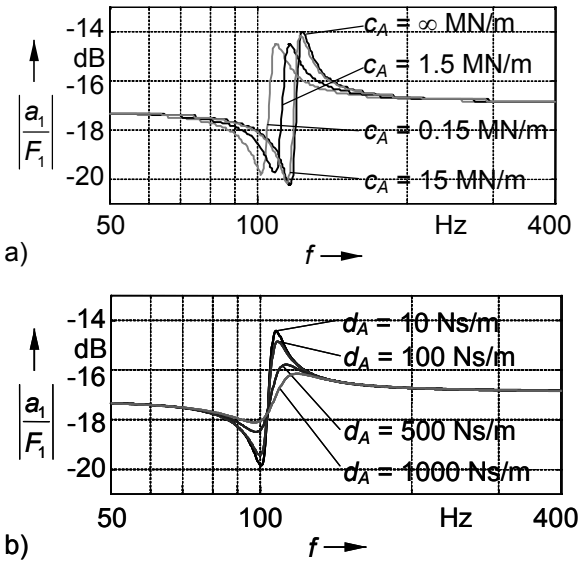

***Figure 6**: Simulated amplitude response $|a_1/F_1|$ of the disturbance transfer function of a semi-active auxiliary mass damper: a) dependance on the active stiffness c_A, b) dependance on the active damping d_A*

4 Active Auxiliary Mass Damper

Passive and semi-active auxiliary mass dampers can only be used to achieve a narrowband damping of the primary force field. Active auxiliary mass dampers achieve broadband damping of the primary force excitation by coupling the auxiliary mass m_{2a} to the host structure m_1 with active materials and a feedback control approach. Based on the dynamic equilibrium of forces acting on the effective mass m_1 shown in Figure 1, its acceleration a_1 is a measure of the compensating effect of the secondary force F_2 originating from the coupled auxiliary mass damper. The goal of active damping is to control the motion of the auxiliary mass m_{2a} with an appropriate electrical driving signal to the active material such that the resulting force $F_2 = m_{2a}a_2$ compensates the immeasurable primary force F_1 and extinguishes the acceleration a_1. This is accomplished in Figure 5a by the dark grey highlighted feedback of the acceleration a_1 to the electrical input of the active material used as actuator.

4.1 Acceleration Sensor

Simple piezoelectric accelerometers consist of a ring-shaped piezoelectric plate that is clamped be-

tween a seismic mass and the sensor case. In the event that the sensor is accelerated the seismic mass exerts a force on the piezoelectric plate. This force, which is proportional to the acceleration, produces an electrical charge due to the direct piezoelectric effect. The electrical charge is conditioned electrically by a charge amplifier and a subsequent low-pass filter. The relationship between the base acceleration a_1 of the sensor case which is to be measured and the output voltage U_{S2} of the sensor electronics for the acceleration sensor is $G_{S2}(p) = U_{S2}(p)/a_1(p)$ and can be expressed as

$$G_{S2}(p) = K_{S2} G_{BA}(p) G_{TP}(p) G_{LV}(p) \tag{20}$$

with the transfer functions of the mechanical subsystem

$$G_{BA}(p) = \frac{1}{\frac{1}{\omega_{rBA}^2} p^2 + \frac{2D_{rBA}}{\omega_{rBA}} p + 1}, \tag{21}$$

of the Butterworth low-pass 2nd-order filter

$$G_{TP}(p) = \frac{1}{\frac{1}{\omega_{rTP}^2} p^2 + \frac{\sqrt{2}}{\omega_{rTP}} p + 1} \tag{22}$$

and of the charge amplifier

$$G_{LV}(p) = \frac{p}{\tau_{LV} p + 1}. \tag{23}$$

The parameters used are the total gain K_{S2}, the resonant frequency ω_{rBA} and the damping ratio D_{rBA} of the mechanical subsystem, the time constant τ_{LV} of the charge amplifier as well as the -3dB cut-off frequency ω_{rTP} of the Butterworth low-pass filter. Table 2 shows the characteristic parameter values of an acceleration sensor.

Parameter	Value	Unit
K_{S2}	0.0313	Vs^3/m
f_{rBA}	45	kHz
D_{rBA}	0.007	-
f_{LV}	1	Hz
f_{rTP}	1	kHz

Table 2: *Characteristic parameter values of an acceleration sensor*

4.2 Closed-Loop Force Compensation

Active compensation of the primary force excitation F_1 can now be achieved by suitable feedback of the measured acceleration a_1 to the input of the controlled current source. In Figure 5b the corresponding acceleration control loop is achieved with G_C as a controller transfer function. So the closed-loop disturbance transfer function results to

$$G_D(p) = \frac{G_{Sa}(p)}{1 - G_{S2}(p) G_C(p) G_A(p) d_M G_{Fa}(p)}. \tag{24}$$

For a P-controller the transfer function is expressed by

$$G_C(p) = K_C. \tag{25}$$

For sufficiently small loop gain this function leads to stable loop behaviour with the aspired broadband rejection characteristic in the frequency domain [9].

Figure 7 shows the dependence of the amplitude response of the disturbance transfer function on the variable K_C. For $K_C > 0$ the behaviour of the disturbance transfer function at first shows an increase in the amplitude response followed by a sharp decline in the region of the anti-resonant frequency of the overall system in passive mode. In this region the damping effect is most significant and diminishes at higher frequencies. Therefore the tuning of the auxiliary mass damper at the dominant frequency component of the primary force excitation is also advisable in the active mode. Unlike the passive auxiliary mass damper even the frequency components of the primary force excitation situated above the dominant frequency component are dampened.

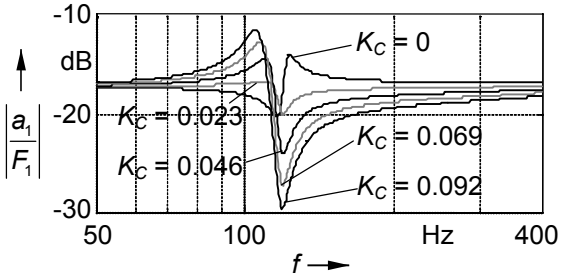

Figure 7*: Simulated amplitude response $|a_1/F_1|$ of the disturbance transfer function of the active auxiliary mass damper.*

5 Coupled Active – Semi-Active Mode (Hybrid Mode)

The characteristic damping behaviour of the actively driven auxiliary mass damper indicates that a combination of the active and semi-active operating modes can be useful when the dominating primary force component undergoes frequency shifts. This hybrid approach is based on the idea of shifting the resonant frequency of the passive auxiliary mass damper so as to effect an electrically controllable variation of the damping behaviour of the active auxiliary mass damper. In combination with suitable signal processing methods and learning algorithms, a hybrid auxiliary mass damper can be brought to adapt its damping behaviour optimally and automatically to time-variant vibration conditions.

The relationship between a_1 and U_{A2} as well as a_1 and F_1 emerging from Figure 5b is expressed as

$$a_1(p) = G_F(p)U_{A2}(p) + G_S(p)F_1(p) \qquad (26)$$

with the transfer functions

$$G_F(p) = \frac{G_A(p)d_M G_{Fa}(p)}{1 - G_A(p)d_M G_{FF}(p)d_P G_{S1}(p)G_E(p)} \qquad (27)$$

and

$$G_S(p) = G_{Sa}(p) + G_{SF}(p)G_{CL}(p)G_{Fa}(p)\,. \qquad (28)$$

Therefore, the disturbance transfer function of the coupled active – semi-active auxiliary mass damper is given by

$$G_D(p) = \frac{G_S(p)}{1 - G_F(p)G_C(p)G_{S2}(p)}\,. \qquad (29)$$

Figure 8a shows the dependence of the amplitude response of the disturbance transfer function on the variable c_A for $d_A = 0$ and $K_C = 0.07$. It is apparent that with decreasing active stiffness c_A the maximum damping in the active mode shifts to lower frequencies and diminishes continuously. This can be explained by the fact that the active displacement s_A produced by a given gain K_C is increasingly "used" by the decreasing active stiffness and thus its contribution to the resulting total displacement diminishes. As Figure 8b shows, the achievement of a pure frequency shift with approximately constant maximum damping effect requires a coordinated variation of the active stiffness c_A and the gain K_C.

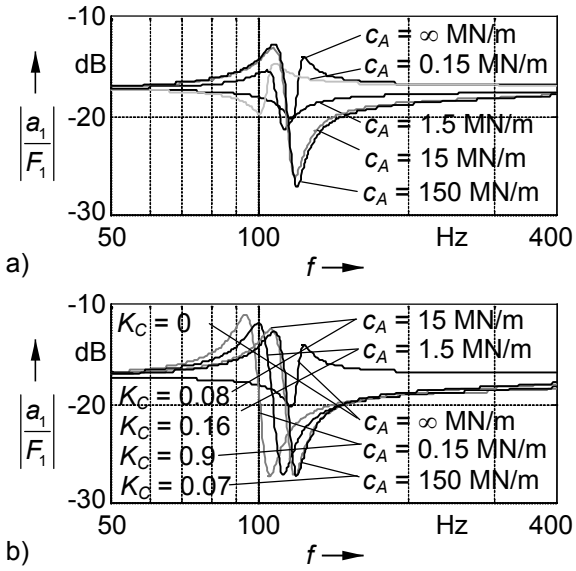

***Figure 8**: Simulated amplitude response $|a_1/F_1|$ of the disturbance transfer function of the coupled active – semi-active auxiliary mass damper: a) variation of the active stiffness c_A with constant K_C, b) variation of the active stiffness c_A with simultaneous variation of K_C*

The functionality of the different operating modes of the presented auxiliary mass damper described above is summarised in Table 3.

	AMD operating mode	Narrow-band	Wide-band	Controllable stiffness and damping	Self-adapting properties
Active materials	Passive	X			
	Active		X		
	Semi-active	X		X	
	Hybrid		X	X	
	Adaptive		X	X	X

***Table 3**: Functionality of the different operating modes of the auxiliary mass damper*

6 Implementation Example

Figure 9 shows a laboratory prototype of an electrically controllable magnetostrictive auxiliary mass damper with displacement amplification represented by the parameter values found in Table 1. The target application of this construction is the active reduction of noise in turbo-prop aircraft by attenuating the vibrations in the cabin structure [11, 13].

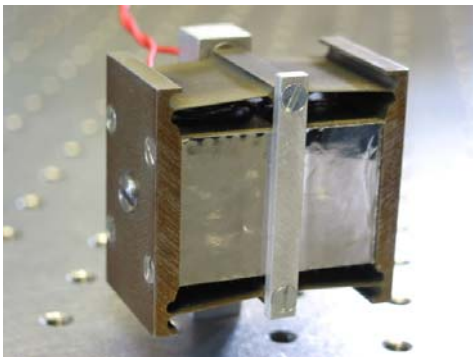

***Figure 9:** Electrically controllable magnetostrictive auxiliary mass damper with displacement amplification*

The vibration spectrum in this application is characterised by three essential components that correspond to the first, second and third rotor blade frequencies situated close to 100 Hz, 200 Hz and 300 Hz. The interesting operating frequency region of the auxiliary mass damper ranges from 50 Hz to 400 Hz. The controllers G_C and G_E used for the experiments have been realised using analogue electronic circuits based on operational amplifiers. An alternative is to implement digital controllers, e.g. with the aid of dSPACE and Matlab/Simulink®.

Rough tuning of the damper is accomplished in the passive mode by adjusting the mechanical preload of the magnetostrictive rods. The anti-resonant frequency for this damper prototype is located at about 111 Hz, see right-hand curve in Figure 10a. A successive increase in the gain factor K_E from zero (passive mode) to values greater than zero (semi-active mode) causes a shift of the anti-resonant frequency down to about 99 Hz.

Compared to the simulation results of Figures 6a, 7, and 8b the measured amplitude responses of the disturbance transfer functions in Figure 10a, 10b and 10d show an increasing damping effect with increasing gain K_E and K_C. This effect might be

caused by the hysteresis losses in the actuator and sensory transfer behaviour of the used active materials growing with the driving amplitude. The controller output is also limited by the power amplifier, and this represents another non-linearity in the system. According to the authors' evaluation, aside from the hysteretic characteristic especially this effect is responsible for a limited range of stability of the control loops in contrast to the idealised linear system model. Therefore, only a qualitative comparison between the measured amplitude responses and the simulated ones is possible here.

Figure 10b shows the amplitude responses of the disturbance transfer function of the auxiliary mass damper in active mode. In accordance with the corresponding simulation results in Figure 7 one can recognise the broadband damping behaviour increasing with the growing gain factor K_C. In the experiments a primary force F_1 of about 12 N was applied.

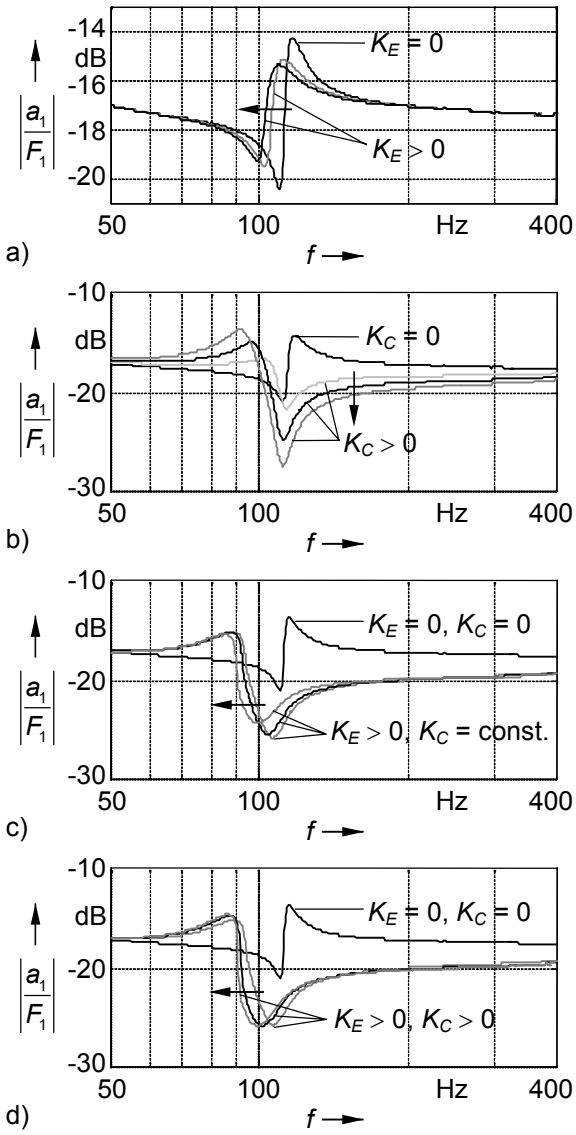

***Figure 10**: Measured amplitude responses $|a_1/F_1|$ of the disturbance transfer function of the auxiliary mass damper: a) semi-active mode, b) active mode, c) and d) coupled active - semi-active mode*

The maximum value for the force F_2 generated in the active case with a stable control loop was about 9 N. So the resulting disturbing force is reduced to about 25% of the original primary disturbance.

Finally Figures 10c and 10d show the amplitude responses of the disturbance transfer function of the auxiliary mass damper in the coupled active - semi-active mode. The behaviour of the real auxiliary mass damper here is also similar to the simulated one. In Figure 10c one can recognise a shift of the point of maximum damping effect to lower frequencies with a contemporaneous reduction of the damping effect for growing K_E, which means decreasing c_A and constant K_C. In Figure 10d one can also see a frequency shift of the point of maximum damping effect for a growing K_E. However, one can recognise that it is possible to compensate a decrease of the maximum damping effect by a corresponding increase of K_C so that only the wanted frequency shift appears in the amplitude responses.

7 Summary

The present paper describes the design and the functionality of a new kind of auxiliary mass damper using active materials. An example is given showing how to realise a coupled active - semi-active damping behaviour on this basis. Constructive optimisation enabled almost the whole damper mass to be effective as seismic mass. The compact construction arising out of this facilitates – in the sense of adaptronics – the integration of the damper into structures capable of oscillation.

In future works the influence of unwanted hysteretic non-linearities in the actuator and sensory transfer behaviour of active materials will be cancelled by means of suitable compensators. Furthermore, there are plans to embed the auxiliary mass damper in an adaptive concept allowing automatic adjustment to the currently present vibration situation.

Literature

[1] Ormondroyd, J.; Denhartog, J. P.: *The Theory of Dynamic Vibration Absorbers*, Transaction of the ASME, Vol. 50, 1928, pp. 9 -22.

[2] Harris, C. H.; Piersol, A. G.: *Harris' Shock and Vibration Handbook*, McGraw-Hill, Berkshire, 2001.

[3] Janocha, H. (Ed.): *Adaptronics and Smart Structures*, Springer, Berlin Heidelberg New York, 1999.

[4] Preumont, A.: *Vibration Control of Active Structures – An Introduction*, Kluwer, Dordrecht Boston London, 2002.

[5] Pagliarulo, P.; Kuhnen, K.; May, C.; Janocha, H.: *Tunable magnetostrictive dynamic vibra-*

tion absorber, Proceedings 9th International Conference on New Actuators, Bremen, 2004, pp. 698-701.

[6] Tichy, J.; Gautschi, G.: *Piezoelektrische Messtechnik*, Springer, Berlin Heidelberg New York, 1980.

[7] Holterman, J.: *Vibration Control of High-Precision Machines with Active Structural Elements*, PhD Thesis, University of Twente, Twente University Press, 2002.

[8] Cedrat Technologies: *Piezo Products Catalogue. Version 3.1*, http://www.cedrat.com, (April 2007)

[9] May, C.; Kuhnen, K.; Pagliarulo, P.; Janocha, H.: *Magnetostrictive Dynamic Vibration Absorber (DVA) for Passive and Active Damping*, Proceedings 5th European Conference on Noise Control, Naples, Italy, 2003, Paper Nr. 159.

[10] Janocha, H. (Ed.): *Actuators – Basics and Applications*, Springer, Berlin Heidelberg New York, 2004.

[11] Franco, F.; Monaco, E.; Lecce, L.: *Vibrations Control Using Hybrid Dynamic Vibration Absorber (HDVAs) Based on Magnetostrictive Active Material*, Proceedings 8th International Conference on New Actuators, Bremen, 2002.

[12] May, C.; Pagliarulo, P.; Janocha, H.: *Optimisation of a magnetostrictive auxiliary mass damper*, Proceedings 10th International Conference on New Actuators, Bremen, 2006, pp. 344-348.

[13] Aurilio, G.; Cavallo, A.; Lecce, L.; Monaco, E.; Napolitano, L.; Natale, C.: *Fuselage Frame Vibration Control Using Magnetostrictive Hybrid Dynamic Vibration Absorbers*, Proceedings 5th European Conference on Noise Control, Naples, Italy, 2003, Paper Nr. 227.

[14] Kuhnen, K.; Pagliarulo, P.; May, C.; Janocha, H.: *Adaptronischer Schwingungsabsorber für einen weiten Einsatzbereich*, at-Automatisierungstechnik, vol. 54, 6/2006, Oldenbourg, Germany, 2006, pp. 294-303.